Available online at www.sciencedirect.com
SCIENCE DIRECT
Journal of Power Sources 158 (2006) 627–634
JOURNAL OF POWER SOURCES
www.elsevier.com/locate/jpowsour

Effect of molecular sieves ZSM-5 on the crystallization behavior of PEO-based composite polymer electrolyte

Jingyu Xi, Xinping Qiu *, Jianshe Wang, Yuxia Bai, Wentao Zhu, Liquan Chen

Key Lab of Organic Optoelectronics and Molecular Engineering, Department of Chemistry, Tsinghua University, Beijing 100084, China

Received 6 June 2005; accepted 10 October 2005
Available online 14 November 2005

Abstract

Polarized optical microscopy (POM) results show that ZSM-5 has great influence on both the nucleation stage and the growth stage of PEO spherulites. Part of ZSM-5 particles can act as the nucleus of PEO spherulites and thus increase the amount of PEO spherulites. On the other hand, ZSM-5 can restrain the recrystallization tendency of PEO chains through Lewis acid–base interaction and hence decrease the growth speed of PEO spherulites. The increasing amount of PEO spherulites, decreasing size of PEO spherulites and the incomplete crystallization are all beneficial for creating more continuous amorphous phases of PEO, which is very important for the transporting of Li^+ ions. An adequate amount of ZSM-5 can enhance the room temperature ionic conductivity of PEO-$LiClO_4$ based polymer electrolyte for more than two magnitudes.

Keywords: Composite polymer electrolyte; PEO; ZSM-5; Spherulites; Ionic conductivity

1. Introduction

All solid-state lithium polymer batteries may be one of the best choices for the future electrochemical power source, characterized by high energy densities, good cyclability, reliability and safety [1,2]. Owing to its potential capability to replace the traditional liquid electrolytes of rechargeable lithium ion batteries, PEO-LiX (X = ClO_4^-, BF_4^-, PF_6^-, $CF_3SO_3^-$, $N(CF_3SO_2)_2^-$, etc.) based polymer electrolytes has received extensive attentions [3–5], since Wright et al. found that the complex of PEO and alkaline salts had ionic conductivity in 1973 [6].

Although PEO-based polymer electrolytes have been studied for more than 30 years, there still exist two opposite opinions on the mechanism of the transporting of Li^+ in PEO matrix. Some researchers support the viewpoint that in PEO-LiX system, crystalline PEO is beneficial for the transporting of Li^+. PEO can form double helix structure through the coordination interactions between the ether O of PEO and Li^+ and then Li^+ can transport in this helix channel through the jump between adjacent coordinate sites [7–9]. Although Bruce et al. have proved that ionic conductivity of the single crystalline PEO_6:$LiXF_6$ (X = P, As, Sb) is much higher than those incomplete crystallization systems [7,8], this method is inconvenient for the large-scale manufacture and process of PEO-based polymer electrolytes. General concepts of the transporting of Li^+ in PEO-based polymer electrolytes are coupled with the local relaxation and segmental motion of PEO chains, of which the conditions can only be obtained when PEO is in its amorphous state [10–14]. Unfortunately, due to the particular structure, PEO often shows much higher crystalline ratios at room temperature, resulting in a very low room temperature ionic conductivity ($\sim 10^{-7}$ S cm^{-1}) of PEO-based polymer electrolytes, which is a drawback for its applications in the consumer electronic market such as cell phone and notebook PC [10].

When the third component, i.e. inorganic fillers, was doped into PEO-based polymer electrolytes to form the composite polymer electrolytes (CPEs), ionic conductivity could be improved obviously [15–17]. Inorganic fillers help to increase the conductivity of CPEs by lowering the reorganize tendency of PEO through Lewis acid–base interactions between ether O of PEO (Lewis base) and Lewis acid sites on the surface of inorganic fillers [10]. XRD, DSC and FT-IR techniques have been widely used to study the crystallization of PEO [10–17]; however, it is hard to obtain the information about how inor-

* Corresponding author. Tel.: +86 10 62794235; fax: +86 10 62794234.
E-mail address: qiuxp@mail.tsinghua.edu.cn (X. Qiu).

0378-7753/$ – see front matter © 2005 Elsevier B.V. All rights reserved.
doi:10.1016/j.jpowsour.2005.10.010

ganic fillers affect the crystallization of PEO only through these techniques.

ZSM-5 molecular sieves have been used in a great deal of catalysis fields, due to its high surface area, special channel structures and strong Lewis acidity [18–20]. In previous work [21–23], we have found that ZSM-5 can obviously enhance ionic conductivity, lithium ion transference numbers and other electrochemical properties of PEO-based polymer electrolyte. In order to elucidate the enhancement mechanisms of ZSM-5, the effect of ZSM-5 on the crystallization of PEO are studied by polarized optical microscopy (POM) technique and the experiment results are discussed in this paper.

2. Experimental

2.1. Materials

Poly(ethylene oxide), PEO, M_w = 1,000,000 (Shanghai Liansheng Chem. Tech.) and $LiClO_4$, A.R. (Shanghai Second Regent Company) were vacuum-dried for 24 h at 50 and 120 °C, respectively, before use. Acetonitrile, A.R. (Shanghai Chemical Regent Company), dehydrate by 4A molecular sieves before use. Al_2O_3 (60 nm, Zhoushan Nano Co. Ltd., China) was vacuum-dried for 24 h at 200 °C prior to use. Li-ZSM-5 was obtained by ion exchange method from H-ZSM-5 (Si/Al = 25, obtained from Nankai University Catalyst Company) and denoted as ZSM-5 [22].

2.2. Preparation of composite polymer electrolytes

The preparation of composite polymer electrolytes involved first the dispersion of PEO and $LiClO_4$ in anhydrous acetonitrile, followed by the addition of filler. The resulting slurry was cast on to a Teflon plate, and then the plate was placed into a self-designed equipment, under the sweep of dry air with a flow rate of 10 L min^{-1}, to let the solvent slowly evaporate. Finally, the result films were dried under vacuum at 50 °C for 24 h to get rid of the residue solvent. These procedures yielded translucent homogeneous self-supporting films of thickness ranging from 100 to 200 μm. The composite polymer electrolytes used in this study were denoted as PEO_{10}-$LiClO_4$/*x*% filler, in which the EO/Li ratio was fixed at 10 and the content of filler, *x*, ranged from 0 to 30 wt.% of the PEO weight.

2.3. XRD measurement

X-ray diffraction (XRD) patterns were recorded by using a Bruker D8 Advance instrument equipped with Cu kα radiation performed at 40 kV and 40 mA. A scan rate of 4.0° min^{-1} over the range of 10–60° (2θ) were used for detecting the characteristic diffraction peak of crystalline PEO.

2.4. DSC analysis

Differential scanning calorimeter (DSC) was carried out on Perkin-Elmer Pyris-1 analyzer at a heating rate of 10 °C min^{-1} from −60 to 100 °C in the heating scan. A flow of nitrogen gas was maintained over the perforated pan to avoid any contact with atmospheric moisture.

2.5. Polarized optical microscopy study

Polarized optical microscopy (POM) was performed using a LEICA-DMLP instrument equipped with a heating stage (Linkam Scientific Instruments Ltd. TMS 94). To test the melting temperature range of PEO spherulites, the sample was heated from room temperature at 5 °C min^{-1}. To study the isothermal crystallization of PEO, all samples were first annealed at 100 °C for 30 min and then quenched rapidly (50 °C min^{-1}) to the given temperature.

2.6. Ionic conductivity

Ionic conductivity of the composite polymer electrolytes was determined by electrochemical impedance spectroscopy (EIS). The electrolyte was sandwiched between two stainless steel (SS) blocking electrodes to form a symmetrical SS/electrolyte/SS cell. The cell was placed into a self-designed oven coupled with a temperature controller. For each temperature, at least 30 min were waited before the impedance response was recorded. The impedance tests were carried out in the 1 MHz to 1 Hz frequency range using a Solartron 1260 Impedance/Gain-Phase Analyzer coupled with a Solartron 1287 Electrochemical Interface.

3. Results and discussion

Polarized optical microscopy (POM) is one of the most effective techniques to study the crystallization of PEO and other polymers [24–26]. Fig. 1 displays room temperature POM images of different samples. For pure PEO (Fig. 1(a)), only few spherulites with the size of 100–200 μm can be observed. PEO spherulites exhibit a typical compact spherulitic morphology and the cross-extinction pattern can be observed clearly. The boundaries of these spherulites are smooth after impingement with adjacent spherulites. After the addition of $LiClO_4$, the amount of spherulites increases and the size of spherulites decreases to about 40–50 μm (Fig. 1(b)). Although the cross-extinction pattern can be observed clearly in PEO_{10}-$LiClO_4$ complex, some dark area can also be observed simultaneously, which corresponds to the amorphous PEO. It is interesting to note that, with the addition of Al_2O_3 and ZSM-5, the amount of PEO spherulites increases further and the average radius of spherulites decreases to only about 20 μm, as shown in Fig. 1(c) and (d), respectively. The cross-extinction pattern of PEO spherulites cannot be observed clearly in PEO_{10}-$LiClO_4$/10%Al_2O_3 and PEO_{10}-$LiClO_4$/10%ZSM-5 because PEO chains are hard to form full spherulites due to the existence of inorganic fillers. The dark area in PEO_{10}-$LiClO_4$/10%Al_2O_3 and PEO_{10}-$LiClO_4$/10%ZSM-5 are larger than that in PEO_{10}-$LiClO_4$, suggesting that the ratio of amorphous PEO in composite polymer electrolytes is higher than that in PEO_{10}-$LiClO_4$.

Fig. 2(a) shows wide angle X-ray diffraction patterns of PEO, PEO_{10}-$LiClO_4$, PEO_{10}-$LiClO_4$/10%Al_2O_3, and PEO_{10}-$LiClO_4$/10%ZSM-5. It is obviously that the characteristic

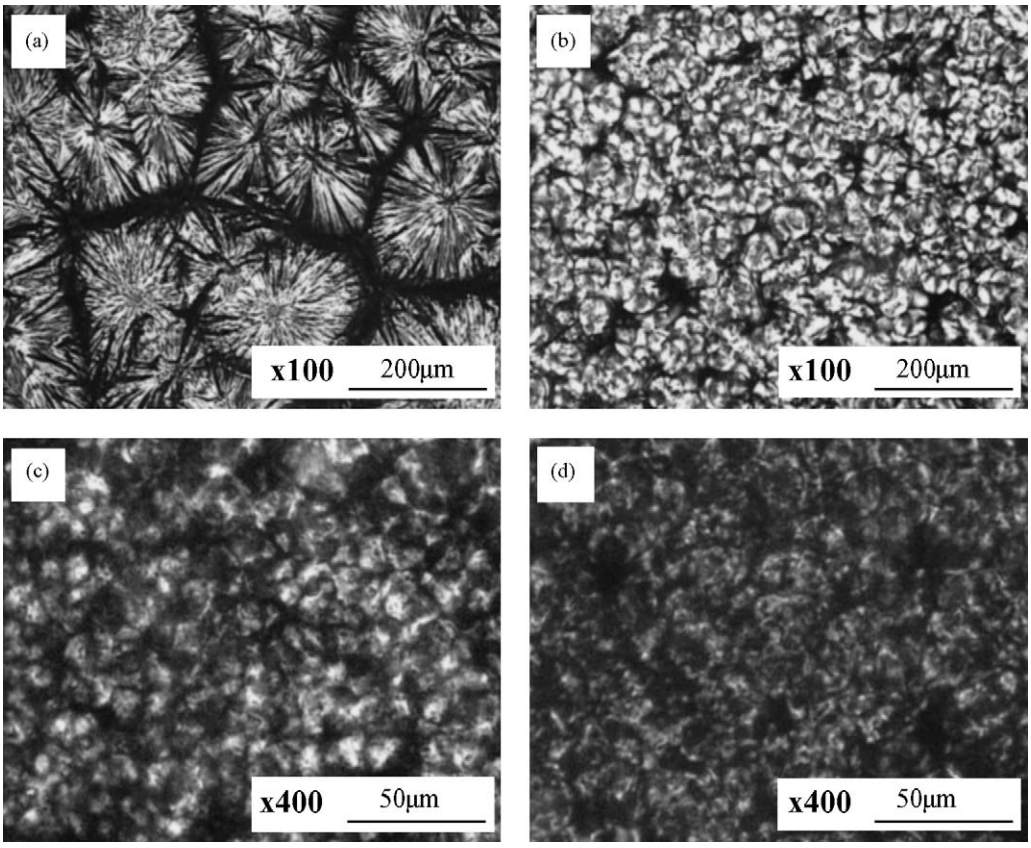

Fig. 1. Polarized optical microscopy (POM) images record at 25 °C for: (a) PEO; (b) PEO_{10}-$LiClO_4$; (c) PEO_{10}-$LiClO_4$/10%Al_2O_3; and (d) PEO_{10}-$LiClO_4$/10%ZSM-5.

diffraction peaks of crystalline PEO ($2\theta = 19$ and 23.5°) become weaker and broader with the addition of $LiClO_4$ and inorganic fillers (Al_2O_3 and ZSM-5). DSC plots of PEO, PEO_{10}-$LiClO_4$, PEO_{10}-$LiClO_4$/10%Al_2O_3, and PEO_{10}-$LiClO_4$/10%ZSM-5 are displayed in Fig. 2(b). For all samples, the endothermic peak between 30 and 70 °C are corresponding to the melting of the crystalline PEO. The crystallinity of PEO (X_c) in all samples is listed in Table 1, which shows that X_c decreases obviously with the addition of $LiClO_4$ and inorganic fillers (Al_2O_3 and ZSM-5). Both XRD and DSC results agree well with the POM images, as shown in Fig. 1.

In situ POM images representing the melting of PEO spherulites in different samples are shown in Fig. 3 and the melting temperature range of PEO spherulites are listed in Table 2.

For pure PEO (Fig. 3(a)), no obvious change in POM image can be observed when temperature is lower than 64 °C. The color of spherulites becomes light and the cross-extinction pattern becomes clearer when temperature reaches 65 °C, corresponding to the melting of spherulites. Finally, PEO spherulites melt rapidly in the temperature range of 65–66 °C. From above results, we can find that the melting temperature range of PEO spherulites is very narrow, indicating that all PEO spherulites grow from the same mechanism. In the case of PEO_{10}-$LiClO_4$ (Fig. 3(b)), the color of spherulites becomes light when temperature reaches 50 °C, corresponding to the melting of spherulites. When temperature reaches 53 °C, the color of spherulites becomes lighter, indicating the faster melting of spherulites. The POM image becomes dark field at 55 °C, corresponding to the completely melting of PEO spherulites. It can be seen from Fig. 3(b) and Table 2 that with the addition of $LiClO_4$, the melting temperature range of PEO spherulites becomes broader, which suggests that $LiClO_4$ has some influence on the mechanism of

Table 1
Thermal properties and room temperature conductivity of the samples

Sample	Melting enthalpy[a] ΔH_m (J g^{-1})	Crystallinity[b] X_c (%)	Conductivity[c] (S cm^{-1})
PEO	135.7	63.5	–
PEO_{10}-$LiClO_4$	83.3	39.0	1.5×10^{-7}
PEO_{10}-$LiClO_4$/10%Al_2O_3	53.6	25.1	9.7×10^{-6}
PEO_{10}-$LiClO_4$/10%ZSM-5	49.7	23.3	1.4×10^{-5}

[a] The data have been normalized to the weight of the PEO matrix.
[b] $X_c = (\Delta H_m^{sample}/\Delta H_m^*) \times 100$, where $\Delta H_m^* = 213.7$ (J g^{-1}) [27].
[c] Test at 25 °C.

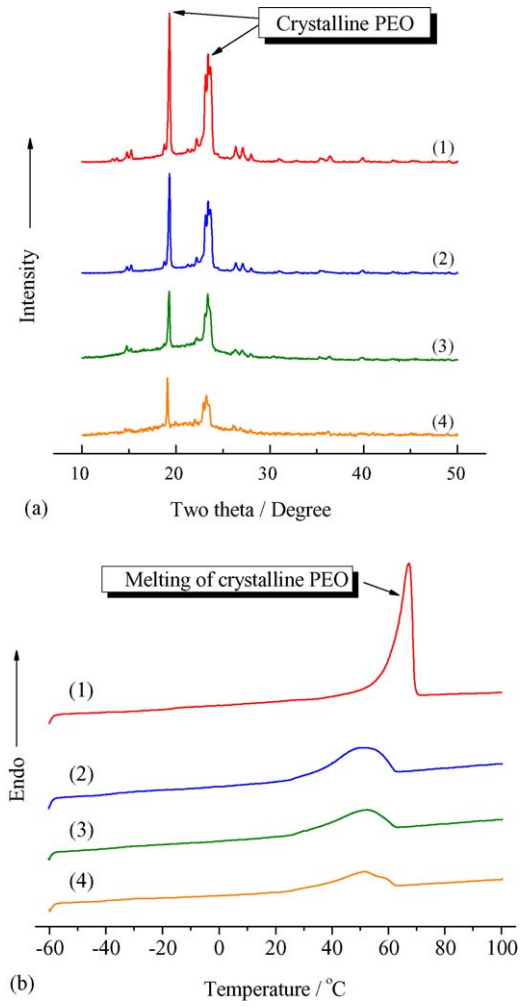

Fig. 2. XRD patterns (a) and DSC plots (b) of the samples. (1) PEO; (2) PEO_{10}-$LiClO_4$; (3) PEO_{10}-$LiClO_4$/10%Al_2O_3; (4) PEO_{10}-$LiClO_4$/10%ZSM-5.

the growth of PEO spherulites. For PEO_{10}-$LiClO_4$/10%Al_2O_3 and PEO_{10}-$LiClO_4$/10%ZSM-5 case (Fig. 3(c) and (d)), the color of spherulites becomes light when temperature reaches 40 °C, corresponding to the melting of spherulites. When temperature reaches about 45 °C, the color of spherulites becomes lighter, corresponding to the rapid melting of spherulites. The POM image becomes dark field at 47–48 °C, indicating the completely melting of PEO spherulites. From above results, we can find that compared with PEO_{10}-$LiClO_4$, the melting temperature range of PEO spherulites in PEO_{10}-$LiClO_4$/10%Al_2O_3 and PEO_{10}-$LiClO_4$/10%ZSM-5 becomes more lower and broader (see Table 2), which suggests that Al_2O_3 and ZSM-5 can also influence the growth of PEO spherulites.

Table 2
Melting temperature range of PEO spherulites obtained from POM analysis

Sample	Melting temperature range (°C)
PEO	65–66
PEO_{10}-$LiClO_4$	50–55
PEO_{10}-$LiClO_4$/10%Al_2O_3	40–48
PEO_{10}-$LiClO_4$/10%ZSM-5	40–47

The effects of Al_2O_3 and ZSM-5 on the crystallization kinetics of PEO are studied by monitoring the isothermal crystallization process of PEO in pure PEO, PEO_{10}-$LiClO_4$, PEO_{10}-$LiClO_4$/10%Al_2O_3 and PEO_{10}-$LiClO_4$/10%ZSM-5, and the obtained in situ POM images are shown in Fig. 4.

In the case of pure PEO, as shown in Fig. 4(a), only one spherulite with clear cross-extinction pattern can be observed at one time during the whole experimental process. The spherulite grows rapidly within few minutes. The formation of spherulites can be divided into two stages, i.e. the nucleation stage and the growth stage. The nucleation stage of spherulites includes homogeneous-nucleation and heterogeneous-nucleation. For pure PEO, only homogeneous-nucleation exists. PEO chains first form nucleus through the local relaxation and segmental motion. Then, these nucleus grows up to form spherulites. We cannot observe the nucleation stage due to the limited instrumental condition. Only few spherulites can be observed in the whole sample, which suggests that PEO chains are hard to form effective nucleus only through spontaneous arrangement. However, these few nucleus begin to grow rapidly as soon as they are formed. It should be noted that in the last image of Fig. 4(a), the diameter of spherulite exceeds 500 μm, which is very larger compared with commonly size (0.5–100 μm) [24].

PEO spherulites grow in PEO_{10}-$LiClO_4$ shows nearly the same POM images as the case of pure PEO (Fig. 4(b)), suggesting the homogeneous-nucleation in the nucleation process of PEO_{10}-$LiClO_4$. The only difference is that the growth speed of PEO spherulites in PEO_{10}-$LiClO_4$ is slower than that in pure PEO. This is because of the coordination interaction between Li^+ and PEO chains, which restrains the motion of PEO chains. PEO spherulites in PEO_{10}-$LiClO_4$ can also form very large size (exceed 300 μm), as shown in the last photo of Fig. 4(b).

PEO spheruhtes in PEO_{10}-$LiClO_4$/10%Al_2O_3 and PEO_{10}-$LiClO_4$/10%ZSM-5 shows completely different crystallization kinetics compared with the case of pure PEO and PEO_{10}-$LiClO_4$, as shown in Fig. 4 (c) and (d), respectively. With the addition of inorganic fillers, the amount of PEO spheruhtes increases. On the other hand, the growth speed of these spherulites decreases obviously.

Based on above isothermal crystallization results, we can find that through the addition of $LiClO_4$ can decrease the growth speed of spherulites, the amount of spherulites do not change, suggesting that $LiClO_4$ can only influence the growth stage of PEO spherulites. After the addition of Al_2O_3 and ZSM-5, the growth speed of spherulites decreases further and the amount of spherulites increases obviously, suggesting that Al_2O_3 and ZSM-5 has great influence on both the nucleation stage and the growth stage of PEO spherulites. It is possible that part of Al_2O_3 and ZSM-5 particles can act as the nucleus of PEO spherulites and thus increase the amount of PEO spherulites. On the other hand, other Al_2O_3 and ZSM-5 particles, which do not act as the nucleus, can restrain the recrystallization tendency of PEO chains through Lewis acid–base interactions and hence decrease the growth speed of PEO spherulites. It can be seen from Fig. 4(c) and (d) that the amount of PEO spherulites in PEO_{10}-$LiClO_4$/10%ZSM-5 is much more than that in PEO_{10}-

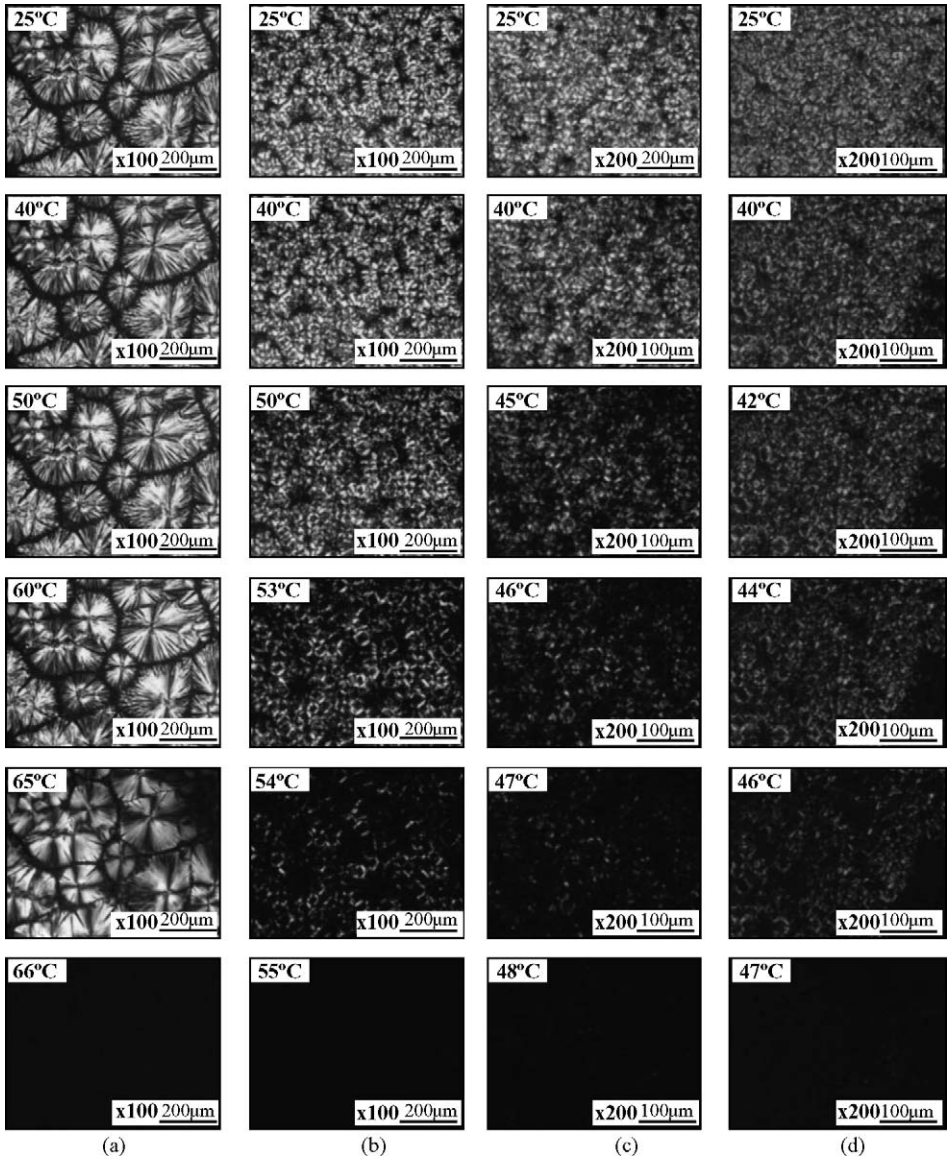

Fig. 3. In situ POM images record during heating scan at a heating rate of 5 °C min^{-1}. (a) PEO; (b) PEO_{10}-$LiClO_4$; (c) PEO_{10}-$LiClO_4$/10%Al_2O_3; (d) PEO_{10}-$LiClO_4$/10%ZSM-5.

$LiClO_4$/10%Al_2O_3, suggesting that ZSM-5 is easy to act as the nucleus of PEO spherulites than Al_2O_3, which should be attributed to the special surface structure of ZSM-5 [18]. In addition, the cross-extinction pattern of PEO spherulites in PEO_{10}-$LiClO_4$/10%ZSM-5 cannot be observed clearly, indicating incomplete crystallization of these spherulites.

Fig. 5 gives the schematic representation of the morphology of PEO spherulites in pristine PEO-$LiClO_4$ and composite polymer electrolyte PEO-$LiClO_4$/ZSM-5. With the addition of ZSM-5, the increasing amount of PEO spherulites, decreasing size of PEO spherulites, and the incomplete crystallization are all beneficial for decreasing the crystallinity of PEO; in other word, increase the ratio of amorphous PEO. In addition, compared with the continuous crystalline phase of PEO formed by the connections of adjacent large PEO spheruhtes in the case of PEO_{10}-$LiClO_4$ (Fig. 5(a)), there exist much more continuous amorphous phase of PEO in PEO_{10}-$LiClO_4$/10%ZSM-5 (Fig. 5(b)), which is very important for the transporting of Li^+ (see green arrow in Fig. 5). R.T. ionic conductivity increases from 1.5×10^{-7} S cm^{-1} of PEO_{10}-$LiClO_4$ to 1.4×10^{-5} S cm^{-1} of PEO_{10}-$LiClO_4$/10%ZSM-5 (Table 1), which supports above discussion successfully.

Time evolution of the crystallinity (obtained from DSC analysis) of PEO (X_c) in PEO_{10}-$LiClO_4$ and PEO_{10}-$LiClO_4$/10%ZSM-5 are shown in Fig. 6. The initial X_c of PEO in PEO_{10}-$LiClO_4$ (25.8%) is much higher than that in PEO_{10}-$LiClO_4$/10%ZSM-5 (12.4%). In addition, the X_c of PEO in PEO_{10}-$LiClO_4$ increases very fast during the whole testing time. On the contrary, the X_c of PEO in PEO_{10}-$LiClO_4$/10%ZSM-5 increases slowly during the whole experiment process and then maintained at a relative low value of about 24% after 1 month. DSC results further prove that ZSM-5 can prevent the recrystallization of PEO effectively, agree with the isothermal crystallization results (Fig. 4).

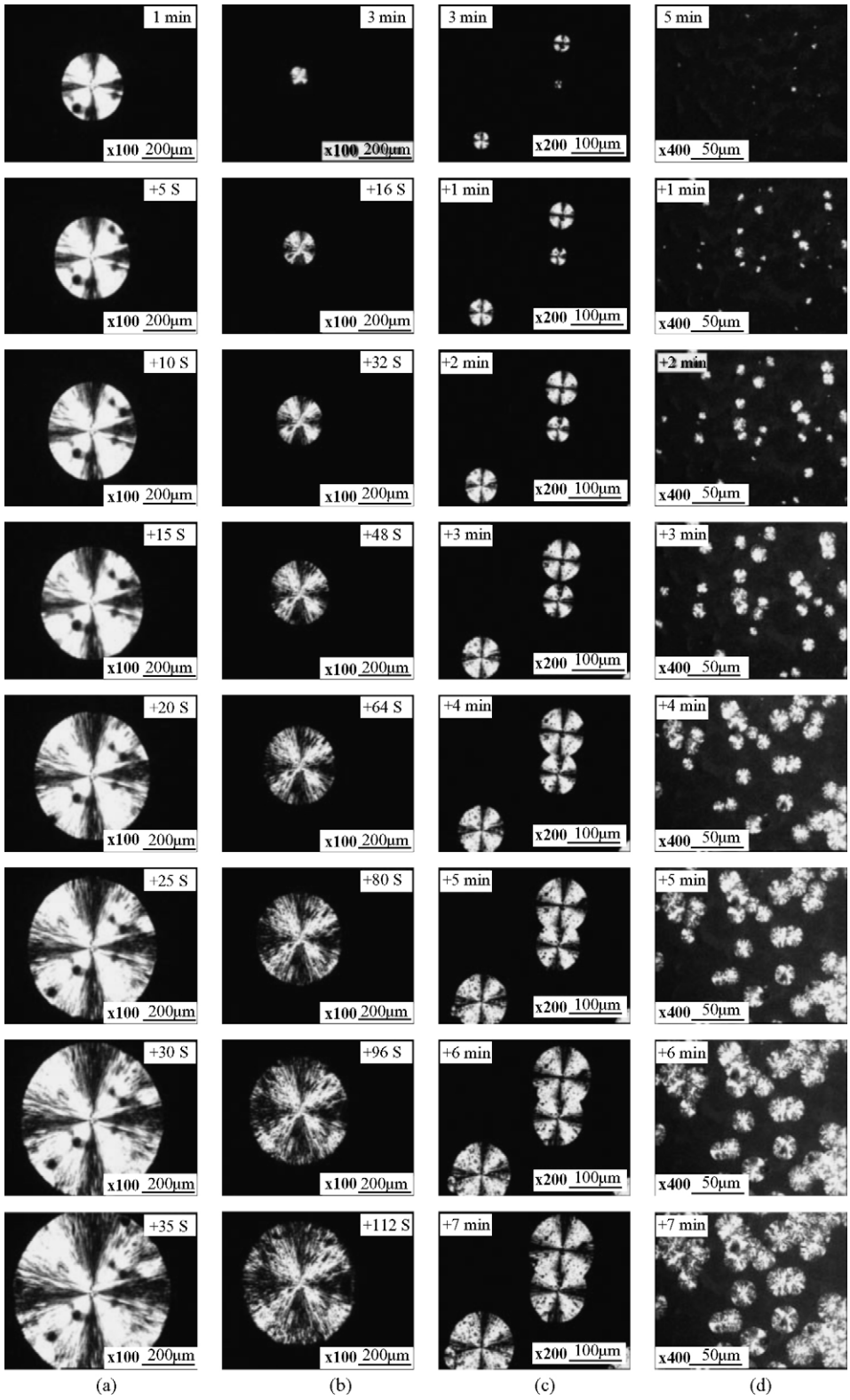

Fig. 4. In situ POM images documenting the growth of PEO spheruhtes from different samples during isothermal crystallization at 45 °C. (a) PEO; (b) PEO_{10}-$LiClO_4$; (c) PEO_{10}-$LiClO_4$/10%Al_2O_3; (d) PEO_{10}-$LiClO_4$/10%Z SM-5.

Fig. 7 displays the time evolution of the R.T. (25 °C) ionic conductivity of PEO_{10}-$LiClO_4$ and PEO_{10}-$LiClO_4$/10%ZSM-5. Prior to test, all samples were vacuum annealed at 100 °C for 24 h and then began the impedance test just after the temperature reached given point. It can be seen from Fig. 4(b) that the initial conductivity of PEO_{10}-$LiClO_4$ after annealing (4.0×10^{-7} S cm^{-1}) is about two times higher than the case without any treatment (1.5×10^{-7} S cm^{-1}); however, PEO_{10}-

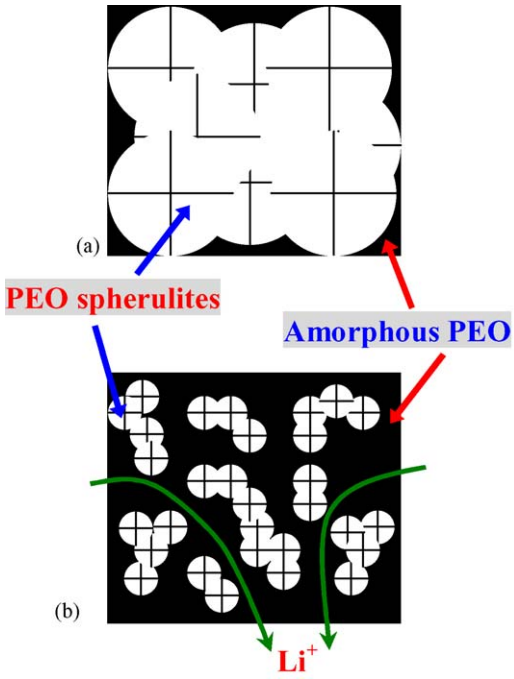

Fig. 5. Schematic representation of the morphology of PEO spheruhtes growth from pristine PEO-$LiClO_4$ (a) and composite polymer electrolyte PEO-$LiClO_4$/ZSM-5 (b).

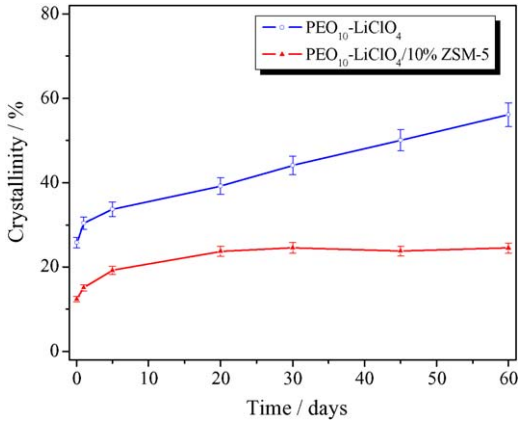

Fig. 6. Time evolution of the crystallinity (X_c) of PEO in PEO_{10}-$LiClO_4$ and PEO_{10}-$LiClO_4$/10%ZSM-5.

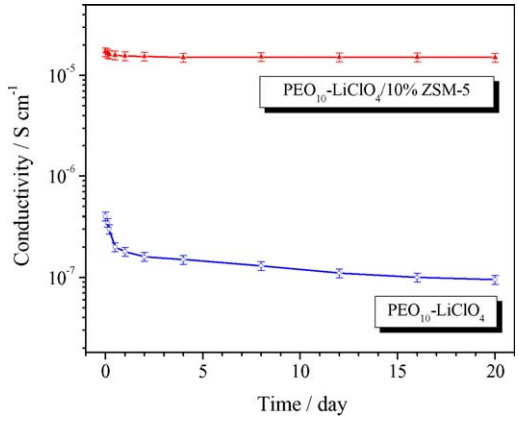

Fig. 7. R.T. (25 °C) ionic conductivity of PEO_{10}-$LiClO_4$ and PEO_{10}-$LiClO_4$/10%ZSM-5 as a function of time.

$LiClO_4$ tends to readily recrystallize and, consequently, its conductivity decreases very fast and then maintained at the value of 1.0×10^{-7} S cm^{-1} after 5 days. PEO_{10}-$LiClO_4$/10%ZSM-5 shows initial ionic conductivity of two magnitudes higher than that of PEO_{10}-$LiClO_4$, and only a small decreasing of ionic conductivity could be detected during the first 2 days. The final conductivity of PEO_{10}-$LiClO_4$/10%ZSM-5 is about 88% compared with its initial value, agree with POM and DSC results.

4. Conclusions

Polarized optical microscopy (POM) technique was used to study the effect of ZSM-5 on the crystallization mechanism of PEO. Experimental results show that ZSM-5 has great influence on both the nucleation stage and the growth stage of PEO spherulites. Part of ZSM-5 particles may act as the nucleus of PEO spherulites and thus increase the amount of PEO spherulites. On the other hand, ZSM-5 can restrain the recrystallize tendency of PEO chains through Lewis acid–base interaction and hence decrease the growth speed of PEO spherulites. The increasing amount of PEO spherulites, decreasing size of PEO spherulites and the incomplete crystallization are all beneficial for creating more continuous amorphous phase of PEO, which is very important for the transporting of Li^+. R.T. ionic conductivity of PEO-based polymer electrolyte can be enhanced by more than two magnitudes with an adequate amount of ZSM-5.

Acknowledgement

This work was financially supported by the State Key Basic Research Program of China (2002CB211803).

References

[1] J.M. Tarascon, M. Armand, Nature 414 (2001) 359.
[2] A.S. Arico, P.G. Bruce, B. Scrosati, J.-M. Tarascon, W.V. Schalkwijk, Nat. Mater. 4 (2005) 366.
[3] V. Chandrasekhar, Adv. Polym. Sci. 135 (1998) 139.
[4] F.M. Gray, Polymer Electrolytes, Royal Society of Chemistry, Cambridge, 1997.
[5] W.H. Meyer, Adv. Mater. 10 (1998) 439.
[6] D.E. Fenton, J.M. Parker, P.V. Wright, Polymer 14 (1973) 589.
[7] Z. Gadjourova, G.Y. Andreev, D.P. Tunstall, P.G. Bruce, Nature 412 (2001) 520.
[8] Z. Stoeva, I.M. Litas, E. Staunton, Y.G. Andreev, P.G. Bruce, J. Am. Chem. Soc. 125 (2003) 4619.
[9] A.M. Christie, S.J. Lilley, E. Staunton, Y.G. Andreev, P.G. Bruce, Nature 433 (2005) 50.
[10] F. Croce, G.B. Appetecchi, L. Persi, B. Scrosati, Nature 394 (1998) 456.
[11] F. Croce, R. Curini, A. Martinelli, L. Persi, F. Ronci, B. Scrosati, J. Phys. Chem. B 103 (1999) 10632.
[12] F. Croce, L. Persi, B. Scrosati, F. Serraino-Fiory, E. Plichta, M.A. Hendrickson, Electrochim. Acta 46 (2001) 2457.
[13] J. Xi, X. Tang, Chem. Phys. Lett. 393 (2004) 271.
[14] C.W. Nan, L.Z. Fan, Y.H. Lin, Q. Cai, Phys. Rev. Lett. 91 (2003) 266104.
[15] J. Zhou, P.S. Fedkiw, Solid State Ionics 166 (2004) 275.
[16] E. Quartarone, P. Mustarelli, A. Magistris, Solid State Ionics 110 (1998) 1.
[17] M.M.E. Jacob, E. Hackett, E.P. Giannelis, J. Mater. Chem. 13 (2003) 1.

[18] A. Corma, Chem. Rev. 97 (1997) 2373.
[19] C.S. Cundy, P.A. Cox, Chem. Rev. 103 (2003) 663.
[20] Ch. Baerlocher, W.M. Meier, D.H. Olson, Atlas of Zeolite Framework Types, fifth ed., Elsevier, Amsterdam, 2001.
[21] J. Xi, S. Miao, X. Tang, Macromolecules 37 (2004) 8592.
[22] J. Xi, X. Ma, M. Cui, X. Huang, Z. Zheng, X. Tang, Chin. Sci. Bull. 49 (2004) 785.
[23] J. Xi, X. Qiu, M. Cui, X. Tang, W. Zhu, L. Chen, J. Power Sources, accepted for publication.
[24] J.H. Yin, Z.S. Mo, Modern Polymer Physics, Science Press, Beijing, 2001.
[25] B. Choi, Solid State Ionics 168 (2004) 123.
[26] B. Choi, Y. Kim, Electrochim. Acta 49 (2004) 2307.
[27] X. Li, S.L. Hsu, J. Polym. Sci. Polym. Phys. Ed. 22 (1984) 1331.